Available online at www.sciencedirect.com
ScienceDirect
Journal of Power Sources 174 (2007) 1104–1108
JOURNAL OF POWER SOURCES
www.elsevier.com/locate/jpowsour

Short communication

Carbon coating via an alkyl phosphonic acid grafting route: Application on TiO_2

U. Lafont [a,*], L. Simonin [a], M. Gaberscek [b], E.M. Kelder [a]

[a] *TU Delft, Delft Chem Tech, NSM, Julianalaan 136, 2628 BL Delft, The Netherlands*
[b] *National Institute of Chemistry, Hajdrihova 19, SI-1000 Ljubljana, Slovenia*

Available online 30 June 2007

Abstract

In the Li-ion battery the electronic conductivity is usually enhanced mixing carbon (black or graphite) with the active cathode material during the electrode preparation. The electronic conductivity is achieved in the system via the percolation of particles. From this point of view, an individual carbon coating of each active material particle is an interesting alternative to enhance conductivity. In this paper, we present a two steps original coating route based on anchoring phenyl phosphonic acid on the surface of anatase TiO_2 and followed by thermal treatment under inert atmosphere. Conductivity tests and galvanostatic measurements at different C-rate have been performed to show the effectiveness of this carbon coating upon lithium insertion.

Keywords: TiO2; Li-ion battery; Alkyl phosphonic acid; Carbon coating; Conductivity

1. Introduction

In the Li-ion battery research field ionic and electronic conductivities are the key parameters of good cycling behaviour upon high rate charging–discharging. In order to enhance the electronic conductivity in cathode materials, the active material is usually mixed with carbon during electrode preparation. For electrode optimisation, minimising the amount of carbon (keeping a good electronic conductivity) is very interesting to enhance energy density. In an optimal case, the carbon particles should surround uniformly each active material particle increasing both ionic and electronic conductivity [1,2]. In such a case, electrons can reach the entire surface of each electro-active particle. On the one hand, this optimal case can be reached only if the carbon particle size is smaller than the active material size as we can see in Fig. 1. On the other hand, from a mass optimisation and electronic conductivity point of view, this method will not be suitable if the carbon particles are bigger than the active nanosized material.

Because of the more frequent use of nanosized particles, the need to have and excellent electronic conductivity and the importance of increasing energy density, an individual carbon coating [3] of each active material particle is a very interesting alternative route. Moreover, for several years, many papers have dealt with carbon coating of cathode materials showing a real improvement in the electronic conductivity and capacity that can be practically utilised. As an example, the effect of a surface carbon coating on the olivine phase $LiFePO_4$ shows that it is possible to render its theoretical capacity even at high rates [4–9].

In this paper, we present a synthesis route using alkyl phosphonic acid as a grafting agent [10–13]. This synthesis approach can be used for all kinds of oxides (TiO_2, Al_2O_3, ZrO_2) metals (Ti, Al, Fe, etc.) and even carbonates ($CaCO_3$). The creation of M–O–P–R bonds will imply some modifications on the grafted materials surface. First, the formation of M–O–P bonds which are strongly covalent. Second, the presence of M–O–P bonds can have a strong inducing effect on the metal atom [14]. Third, we will obtain a monoatomic layer of phosphorus at the surface. We chose to use anatase TiO_2 as an active material that can reversibly insert lithium with a capacity of 150 mAh g^{-1} at 1.755 V (versus Li/Li^+) corresponding to the formation of the titanate phase $Li_{0.55}TiO_2$. This behaviour is observed for micrometer-sized anatase but recent studies [15] show that nanometer-sized anatase can insert more lithium and reach, in some cases, the composition Li_1TiO_2 (capacity of 335 mAh g^{-1}). Besides, it is known from previous studies [16] that grafting of alkyl phosphonic acid on TiO_2 can be easily achieved. The linking process will be (bi-)tridendate (Fig. 2)

* Corresponding author.
E-mail address: u.lafont@tudelft.nl (U. Lafont).

0378-7753/$ – see front matter © 2007 Elsevier B.V. All rights reserved.
doi:10.1016/j.jpowsour.2007.06.186

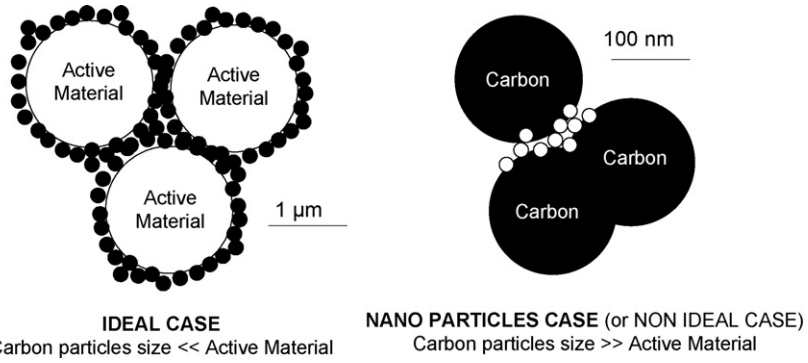

Fig. 1. Percolation procedure between carbon and active material depending on the particle size.

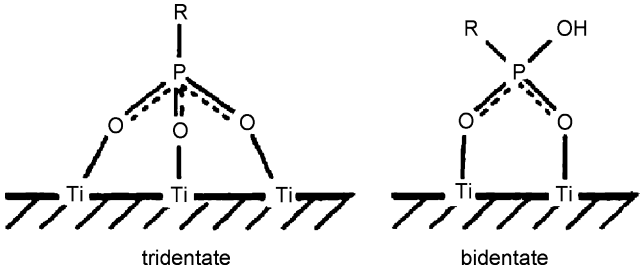

Fig. 2. Anchoring mode of alkyl phosphonic acid on TiO_2.

leading to a strong and stable anchoring. The first step of this coating process is driven by the condensation of the alkyl phosphonic acid molecules with the hydroxyl groups of the TiO_2 surface.

The second step of this coating consists in a thermal treatment under inert atmosphere in order to form a carbon shell by calcination of the alkyl groups. It has been shown by Doeff et al. [17], that the carbon structure at the surface can affect the electrochemical performance of the coated material. It seems that Csp^2 instead of Csp^3 hybridization type carbon enhances performance of the coated sample and reduces the average amount of carbon needed for the same electrochemical characteristics. From this point of view we chose phenyl phosphonic acid as a grafting material (Fig. 3).

2. Synthesis

The anatase TiO_2 source (AK1 Tronox, Keer-McGee Chemical) has an average particle size of 25 nm and a surface area of 90 $m^2\,g^{-1}$. In a typical synthesis process, phenyl phosphonic acid (Aldrich) is dissolved in dichloromethane and TiO_2 is added to this mixture under stirring at room temperature. The resulting mixture is then stirred 24 h at room temperature. The amount of dichloromethane used is 20 ml g^{-1} of TiO_2. The amount of phenyl phosphonic acid used corresponds to fivefold excess relative to the amount needed for full surface coverage of the TiO_2 particles (assuming an area of 24 $Å^2$) by alkyl phosphonic acid molecules. The grafted TiO_2 particles are recovered by filtration and washed with dichloromethane then acetone and finally with a mixture of water/acetone (50/50 %vol). The as-synthesized grafted TiO_2 powder is dried overnight in an oven at 80 °C. In order to create a carbon coating by degradation of the phenyl groups, the as-synthesized powder is thermally treated for 12 h under Ar atmosphere at 300 or 500 °C.

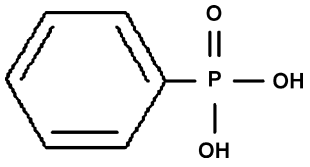

Fig. 3. Phenyl phosphonic acid structure.

3. Characterization

Structural characterizations have been made using powder X-ray diffraction with a Bruker D8 DiffractPlus diffractometer using Cu Kα radiation. Transmission electron microscopy (TEM) was performed using a FEI Tecnai TF20 electron microscope equipped with EELS (Electron Energy Loss Spectroscope) for element analysis. ^{31}P and ^{13}C solid state NMR has been performed using a Bruker Avance 400 apparatus. For conductivity measurements the samples were pressed into pellets then placed into a gas-tight quartz tube equipped with four shielded electrical Pt wires. The contacts to samples were made using a Pt paste. The quartz tube was inserted into a furnace with controlled temperature (±1 K). The atmosphere in the tube was controlled by channelling the appropriate gas flow through it. The impedance spectra were recorded using a Solratron FRA 1260 combined with an EG&G 283 Potentiostat/Galvanostat. The frequency range was 100 kHz to 0.1 Hz and the excitation amplitude was 10 mV (r.m.s.). Electrochemical tests were performed in Swagelok type cells with pure metal Li (Aldrich) as an anode using 1 M $LiPF_6$ EC:DMC 2:1 (Mitsubishi Chemical) as an electrolyte and Whatman Glass fibber as separator. The cells were assembled in a He filled glove box. These tests were performed with a Maccor S4000 tester in a galvanostatic mode using different constant current rates. The same cell is discharged–charged at different current rates during five cycles following this order: 7.5, 15, 30, 75, 150, 750, 1500 and 7.5 mA g^{-1}.

4. Results and discussion

As we can see from the XRD patterns presented Fig. 4, the crystalline structure of the starting material does not change

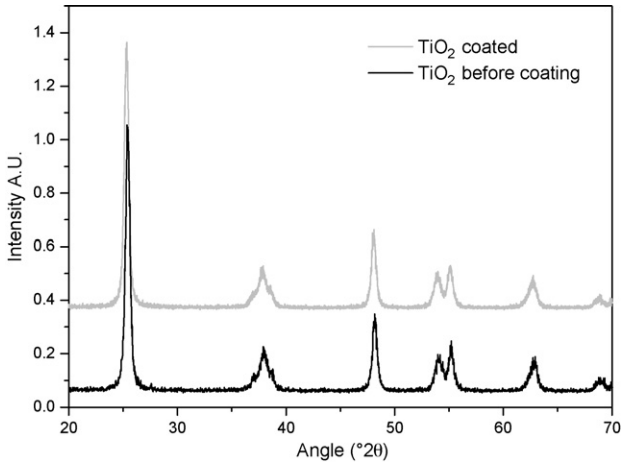

Fig. 4. XRD pattern of TiO_2 before and after the coating process.

after the grafting and thermal treatment process. Nanocrystalline TiO_2 anatase is still present. The diffraction peaks show the same width and relative intensities. The phenyl phosphonic acid anchoring procedure does not affect the crystalline structure and texture of the starting support. Moreover, no extra phases appear: no metal phosphate phase can be seen due to a dissolution–precipitation process that usually competes with the surface modification process at high temperatures of synthesis and high alkyl phosphonic acid concentrations.

This absence of metal phosphate phase is proof that self-condensed alkyl phosphonic molecules are absent by formation of P–O–P bonds. In this case, surface modification of TiO_2 particles by grafting phenyl phosphonic acid molecules leads to the formation of a monolayer. As we can see in Fig. 5, ^{31}P MAS NMR spectroscopy also confirms the presence of the grafted phosphonic acid on the surface of TiO_2 after thermal treatments. The peaks are in the R_3P chemical shift range. The presence of two peaks can be explained by the inhomogeneity of the anchoring process of the phosphonic acid on the surface (presence of bi and tridentate ligands).

The ^{13}C MAS NMR also confirms the presence of grafted phosphorus atoms on the surface of TiO_2 showing a resonance at 57.7 ppm corresponding to the carbons linked to the phosphorus atoms. The spectrum does not show any aromatic carbon. The thermal treatment leads to the degradation of the phenyl groups as we can see with the presence of the resonance at 17.2 ppm due to aliphatic carbons.

The HRTEM pictures, like X-ray diffraction for crystal structure, confirm that this grafting process do not affect the support (i.e. TiO_2) from a textural and morphological point of view (Fig. 6). The particles are still well crystallised and homoge-

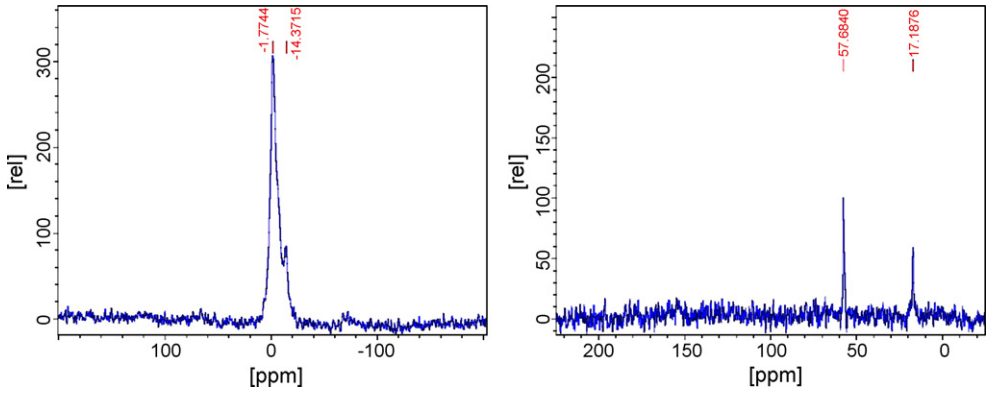

Fig. 5. ^{31}P (left) and ^{13}C (right) NMR spectra.

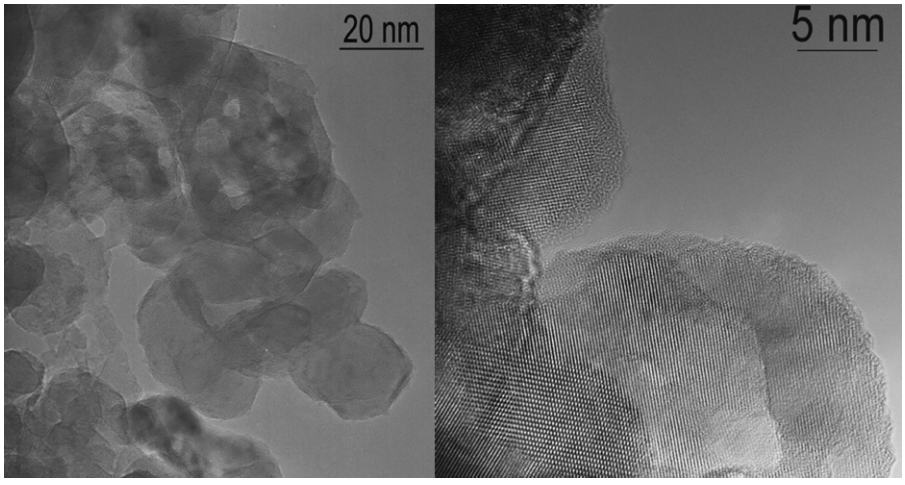

Fig. 6. HRTEM micrographs of grafted TiO_2 (left). High magnification images of the area studied with EELS (right).

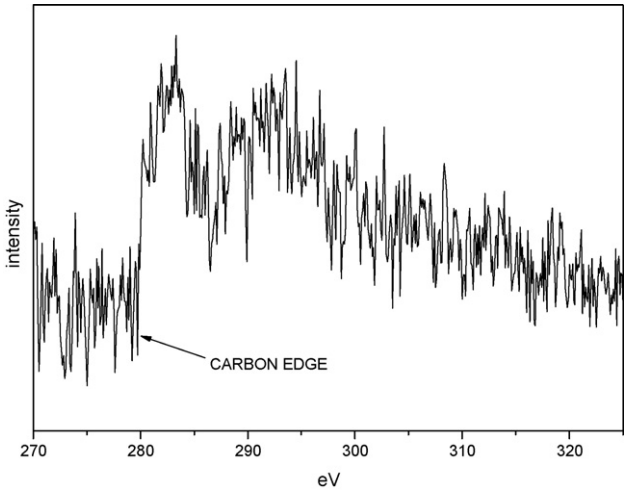

Fig. 7. EELS spectrum of the TiO_2 grafted sample after thermal treatments showing the carbon edge.

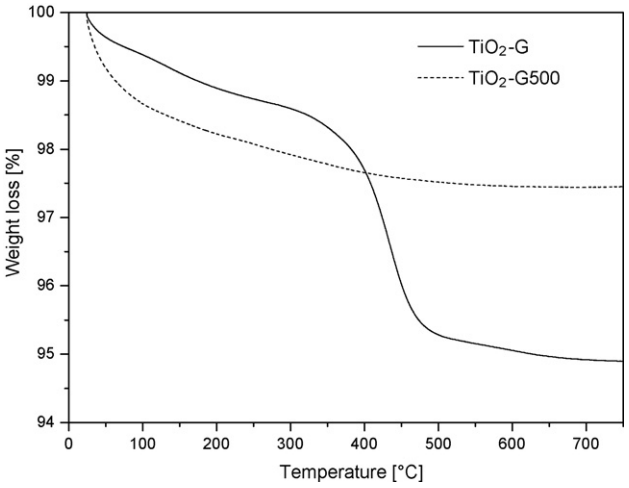

Fig. 8. TGA measurements under $N_2 + 10\%$ O_2 of the TiO_2 material as-grafted (TiO_2-G) and thermally treated under Ar at 500 °C (TiO_2-G500).

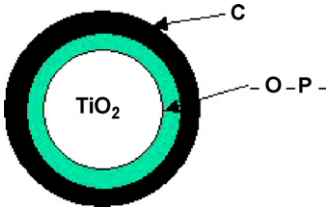

Fig. 9. The core-shell model resulting from the coating process via phenyl phosphonic acid grafting showing the monoatomic layer of phosphorus atoms.

neous in size. From this analysis, the TiO_2 particles do not present a visible shell of carbon. The minimal size of the shell resulting from the anchoring of phenyl phosphonic acid will be less than 0.500 pm (taking into account the size of the P–C bond (0.187 pm) and the phenyl (0.280 pm)). Moreover, this shell consists of an atomic layer of phosphorous atoms and amorphous carbon on it. From this point of view, it is quite difficult to show the existence of a shell formation by TEM. Nevertheless, EELS shows the presence of carbon as we can see in Fig. 7 by the presence of the edge around 280 eV.

From all these characterizations, it is clear that the TiO_2 nanoparticles of anatase are coated with a monoatomic layer of phosphorus atoms via Ti–O–P bonds. The carbon atoms are linked to the surface via the phosphorus atoms that act like coupling agents with the support via P–C bonds. The initial phenyl group do not exist anymore and are replaced by aliphatic carbons upon thermal treatments. According to the maximum amount phosphorus that can be grafted on TiO_2 ($5\,P\,nm^{-2}$) [11] the percentage of carbon in this material will be 5% maximum. From TGA measurements (Fig. 8) the weight loss is around 4% between 200 and 500 °C. This weight loss is due to the decomposition of the aromatic species grafted on the surface of the material.

For the thermally treated material, the weight loss is around 2% and stable after 500 °C and can be related to the carbon percentage in the material. The result of the coating process can be seen in Fig. 9.

To see the advantage of this coating on the electrochemical behaviour, we perform conductivity measurements from 25 to 300 °C under Ar atmosphere. In Fig. 10 we can see the conductivity data as a function of temperature for three samples: pure TiO_2, TiO_2 grafted and thermally treated at 300 °C (denoted as TiO_2-G300) and TiO_2 grafted and thermally treated at 500 °C (denoted as TiO_2-G500). We can see that pure TiO_2 and TiO_2-G300 present almost the same Arrhenius plots, whereas TiO_2-G500 exhibits significantly higher conductivity (around two orders of magnitude) at all temperatures. However, the activation energy is similar for all samples around $82.8\,kJ\,mol^{-1}$ (0.86 eV). This behaviour is quite surprising, assuming that pure and grafted samples should have different conduction mechanisms giving different activation energies. Galvanostatic measurements have been performed using different current discharge–charge, as we can see in Fig. 11, in order to see the benefits of the carbon coating upon lithium insertion and cycling stability. Every five cycles, the current is increased. For the first cycles, the characteristics of the pure TiO_2, TiO_2-G300 and TiO_2-G500 are quite the same at low current rates ($7.5\,mA\,g^{-1}$).

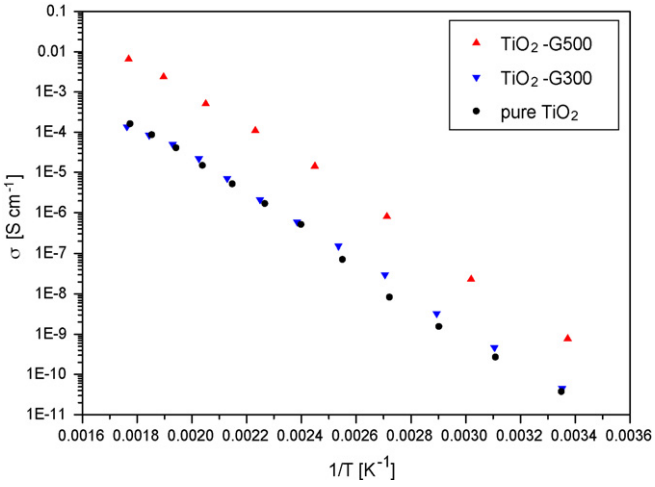

Fig. 10. Conductivity data as a function of temperature (Arrhenius plots) of pure TiO_2, TiO_2-G300 and TiO_2-G500.

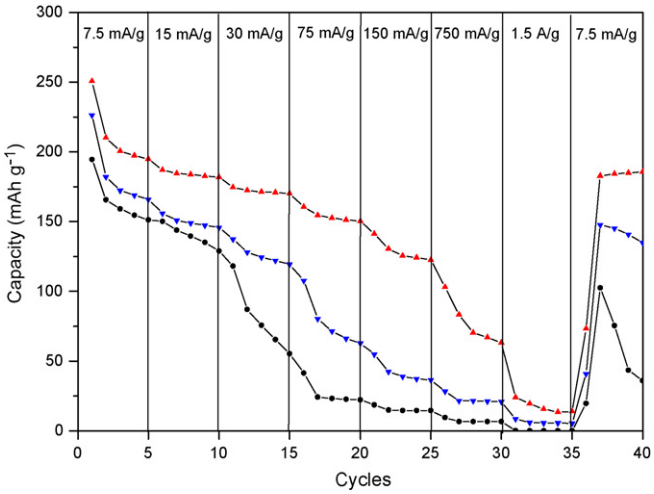

Fig. 11. Evolution of the capacity for each material ((▲) TiO_2-G500 (▼) TiO_2-G300 and (●) pure TiO_2)) as a function of the cycles for different current of discharge–charge.

Table 1
Capacity in mAh g^{-1} after five cycles for each material at different discharge–charge currents (mA g^{-1})

Current (mA g^{-1})	7.5	15	30	75	150	750	1500
Pure TiO_2	150	130	55	22	15	6	0
TiO_2-G300	165	145	120	62	35	20	5
TiO_2-G500	195	180	170	150	125	63	13

After the five first cycles at 7.5 mA g^{-1}, we can see rapid capacity fading: pure TiO_2 and TiO_2-G300 gave practically the same capacity (155 mAh g^{-1}), whereas TiO_2-G500 exhibits a significantly higher capacity (195 mAh g^{-1}) corresponding to $Li_{0.88}TiO_2$. Initially, at current rate of 15 mA g^{-1}, pure TiO_2 and TiO_2-G300 still have similar capacities (145 mAh g^{-1}) but after three cycles pure TiO_2 starts to lose more capacity. In contrast, for TiO_2-G500, the capacity is still high and stable (180 mAh g^{-1}).

For the 30 mA g^{-1} current, the capacity of pure TiO_2 sample drops dramatically to 55 mAh g^{-1}, whereas for TiO_2-G300 and TiO_2-G500 materials the capacity is stable at 120 mAh g^{-1} and 170 mAh g^{-1}, respectively. With a discharge–charge current of 75 mA g^{-1}, the capacity for pure TiO_2 dropped to 22 mAh g^{-1} after five cycles. However, TiO_2-G500 can still recover 150 mAh g^{-1} reversibly. The TiO_2-G300 material shows dramatic capacity fading from 75 to 62 mAh g^{-1}. Using a discharge–charge current of 150 mA g^{-1}, all samples show stable cycling with a capacity for pure TiO_2, TiO_2-G300 and TiO_2-G500 of 15, 35 and 125 mAh g^{-1}, respectively. For a 750 mA g^{-1} current rate, the capacity of the TiO_2-G500 drops to 63 mAh g^{-1}. The capacity for the two other materials is still stable but very low. Finally, for a 1500 mA g^{-1} current rate, the capacity of all samples is below 10 mAh g^{-1}. An overview of the capacities is summarized in Table 1.

The last five cycles presented on Fig. 10 have been performed with a current of 7.5 mA g^{-1}. We can see that only the coated materials can recover their initial capacity. The capacity of this anatase material is higher than the classical capacity of anatase TiO_2 (150 mAh g^{-1}) corresponding to the formation of $Li_{0.55}TiO_2$. The TiO_2-G500 material recovers a capacity of 185 mAh g^{-1}. The other two samples cannot deliver the currents and maintain a practical capacity. Only TiO_2-G500 seems to be able to deliver high current and recover completely after this high power demand. The coating process seems to drastically enhance the stability of the material upon lithium insertion. Clearly, all samples show a dramatic drop in the capacity at higher current. This drop appears for pure TiO_2 at 30 mA g^{-1}, for TiO_2-G300 at 75 mA g^{-1} and TiO_2-G500 at 750 mA g^{-1} reflecting the benefits of the coating.

5. Conclusion

The carbon coating of TiO_2 nanoparticles using phenyl phosphonic acid followed by special thermal treatments is efficient. NMR and EELS show that the TiO_2 particles have carbon present on their surface. The monoatomic layer of phosphorus is needed and ensures a covalent bond between the TiO_2 core and C shell forming Ti–O–P–C bonds. Conductivity measurements indeed showed an improvement in electronic conductivity for the 500 °C treated material. This conductivity improvement came with a better capacity retention at high current densities and cycling stability. Moreover, this coating process can be applied to all oxides and do not require very high temperature.

Acknowledgment

The authors would like to thank the European Network of Excellence ALISTORE for funding.

References

[1] R. Dominko, M. Gaberscek, J. Drofenik, M. Bele, J. Jammik, Electrochem. Acta 48 (2003) 3709.
[2] R. Dominko, M. Gaberseck, J. Drofenik, M. Bele, S. Pejovnik, J. Jamnik, J. Power Sources 119–121 (2003) 770.
[3] J.M. Tarascon, et al., Dalton Trans. (2004) 2988.
[4] M. Armand et al., US Patent 2004,033,360, 2004.
[5] R. Dominko, et al., J. Electrochem. Soc. 152 (2005) A607.
[6] R. Dominko, et al., J. Electrochem. Soc. 152 (2005) A858.
[7] H. Huang, et al., Electrochem. Solid-State Lett. 4 (2001) A170.
[8] K.F. Hsu, et al., J. Mater. Chem. 14 (2002) 2690.
[9] Z.H. Chen, et al., J. Electrochem. Soc. 149 (2002) A1184.
[10] G. Guerrero, PhD Thesis, University of Montpellier, 2 (2000).
[11] G. Guerrero, et al., J. Mater. Chem. 11 (2001) 3161.
[12] P.H. Mutin, et al., C. R. Chimie 6 (2003) 1153.
[13] P.H. Mutin, et al., J. Mater. Chem. 15 (2005) 3761.
[14] A.K. Padhi, K.S. Nanjundaswamy, C. Masquelier, S. Okada, J.B. Goodenough, J. Electrochem. Soc. 144 (1997) 1609.
[15] M. Wagemaker, D. Lützenkirchen-Hecht, A.A. van Well, R. Frahm, J. Phys. Chem. B 108 (2004) 12456.
[16] G. Guerrero, P.H. Mutin, A. Vioux, Chem. Mater. 13 (2001) 4367.
[17] M.M. Doeff, Y. Hu, F. Mc Larnon, R. Kostecki, Electrochem. Solid State Lett. 6 (2003) A207.